Thermochimica Acta, 137 (1989) 293–306
Elsevier Science Publishers B.V., Amsterdam – Printed in The Netherlands

THERMAL CHARACTERIZATION OF THE NEAR-SURFACE OF POLYCRYSTALLINE METAL OXIDES, NiO, CuO AND MgO, BY EMANATION THERMAL ANALYSIS USING ^{226}Ra AS PARENT ISOTOPE

TADAO ISHII

*Department of Applied Chemistry, Faculty of Engineering, Hokkaido University,
Sapporo 060 (Japan)*

(Received 17 February 1988)

ABSTRACT

The thermal characterization of the surface layers of polycrystalline metal oxides, NiO, CuO and MgO (which were prepared by the decomposition of their basic carbonates or hydroxides), was studied by means of emanation thermal analysis (ETA) using a surface impregnation method with ^{226}Ra as parent isotope under a controlled temperature programme of 10 °C min^{-1} in a flow of nitrogen. The ETA results provided useful information on the thermal behaviour of grain boundaries; this could not be followed by the conventional thermoanalytical methods such as thermogravimety, differential thermal analysis, high temperature X-ray diffraction, etc.

INTRODUCTION

The author has already reported on the applications of emanation thermal analysis (ETA) using ^{226}Ra as parent isotope for the thermal characterization of iron oxide and aluminium oxide powders [1–3] and for the surface reactivity of metal oxide powders in the systems TiO_2–$BaCO_3$ and Fe_2O_3–Al_2O_3 [4,5]. A comprehensive review on the applications of the ETA technique using mainly ^{228}Th nuclide for various metal oxides has been reported by Balek [6].

In this paper, the ETA technique (using a surface impregnation method with ^{226}Ra as parent isotope) was applied to follow the thermal behaviour of the surface layer of the polycrystalline metal oxides, NiO, CuO, Cu_2O and MgO (prepared by the decomposition of their basic carbonates or hydroxides).

EXPERIMENTAL

Materials

Two nickel oxides, NiO(C-1450) and NiO(H-1450), were prepared from basic nickel carbonate and nickel hydroxide by calcining to 1450 °C under

0040-6031/89/$03.50

the conditions of the ETA tests (heating rate, 10 °C min^{-1}; nitrogen flow, 50 ml min^{-1}). Furthermore, five nickel oxides in two series, NiO(C-500), NiO(C-850), NiO(H-500), NiO(H-850) and NiO(H-1100), were prepared from basic nickel carbonate (C-series) and nickel hydroxide (H-series) by calcining at 500, 850 and 1100 °C for 1 h in air. The basic nickel carbonate, $NiCO_3 \cdot 2Ni(OH)_2 \cdot 4H_2O$, was commercial reagent grade of < 200 mesh size (Kanto). The nickel hydroxide, $Ni(OH)_2$, was prepared by precipitation from a mixture of 0.5 M $NiSO_4$ and 1 M NaOH solutions. After ageing the precipitate for 45 h at 25 °C, the $Ni(OH)_2$ obtained was washed, filtered, dried and ground to pass through a 200 mesh sieve.

Copper oxides, CuO and Cu_2O, were prepared from commercial basic cupric carbonate (Kanto), $CuCO_3 \cdot Cu(OH)_2 \cdot H_2O$, by calcining to 800 and 1050 °C under the conditions of the ETA tests shown above.

Two magnesium oxides, MgO, were prepared from commercial basic magnesium carbonate (Kanto), $4MgCO_3 \cdot Mg(OH)_2 \cdot 5H_2O$, and magnesium hydroxide (Kanto), $Mg(OH)_2$, by calcining to 1500 °C under the conditions of the ETA tests shown above. Commercial magnesium oxide (Kanto) was also used.

Apparatus and procedures

The apparatus used for the ETA tests was a Netzsch ETA 403 - STA 409 type for simultaneous ETA–TG–DTA measurements. The standard experimental conditions were as follows: sample weight, 100 mg; nitrogen carrier gas, flow rate 50 ml min^{-1}; heating and cooling rates, 10 °C min^{-1}; threshold, 2 MeV; time constants, 100 s for NiO and CuO, and 300 s for MgO. The sample powders were labelled by a surface impregnation method using an aqueous ^{226}Ra solution (4–10 $\mu Ci\ ml^{-1}$) and were dried by heating under an infrared lamp without further washing of the surface of the labelled powders. Before being used for ETA experiments, in both the first and repeated runs, the dried labelled samples were stored, for periods exceeding one month until a radioactive equilibrium state was reached. The parent nuclide ^{226}Ra was adsorbed on the surface and the daughter inert gas atom ^{222}Rn was formed by α decay and was introduced into the surface layer (< 50 nm thick) by the recoil energy [7].

Interpretation of ETA curves

Information obtained from the ETA experiments can be correlated with the thermal behaviour of the near-surface of the powder (< 50 nm thick) during a temperature rise. The implications of various observed ETA peaks have already been considered in refs. 1–5 on the basis of studies by Balek [8], Matzke [9] and Jech and Kelly [10].

The characteristic peaks in the ETA curves observed in this work were divided into two main groups: group I, those due to E_p (the emanating power caused by the diffusion of radon into the intergranular space, open pores, etc.) at temperatures lower than $T_s=(0.4–0.5)\ T_m$; group II, those due to E_d (the emanating power due to diffusion of radon through the solid matrix of the dispersed material) at temperatures higher than T_s. T_m is the absolute melting temperature of the material. The onset temperatures T_s of gas release due to E_d are similar to those of self-diffusion of the lattice ions. The values of T_s are estimated to be 616–839 °C for NiO (T_m=2223 K), 295–438 °C for CuO (T_m=1421 K), 328–479 °C for Cu_2O (T_m=1503 K) and 968–1279 °C for MgO (T_m=3103 K). The value of T_m for CuO is unreliable because the decomposition to Cu_2O occurs above 900 °C (Fig. 9).

The ETA peaks corresponding to groups I and II are hereafter represented by peaks I and II, respectively. In many cases, peak II was split into two peaks, IIa and IIb. It is thought that peak IIa corresponds to gas release from the defect structures such as the grain boundaries (dislocation) or the amorphous part present in the surface layer. On the other hand, a process with a maximum at 700–760 °C for α-Al_2O_3 (T_s = 656–889 °C) is known to be connected with the amorphous–crystalline transition [10]. Such a peak located at around the temperature T_s was denoted by peak I′. Radiation-induced amorphousness has been studied [6], but this will not be a problem here because of the use of low doses. Peak IIa is shifted to higher temperature by heating, and closely approaches peak IIb, which is thermally stable over the range of experimental temperatures.

RESULTS AND DISCUSSION

Nickel oxides

Nickel oxides from carbonate

Figure 1 shows the ETA–TG–DTA curves of basic nickel carbonate in the temperature range 25–1450 °C, including the decomposition processes at temperatures below 500 °C. In the first run (run 1), the TG–DTA curves show the decomposition behaviour, with good correspondence with the ETA peaks. In the second run (run 2) for nickel oxide, NiO(C-1450), which was formed in run 1, the ETA peaks below 500 °C disappear, and two peaks, peak IIa (including peak I) starting at about 500 °C and peak IIb with a maximum at 1250 °C, appear. In run 3, the ETA curve agrees with that in run 2. This means that nickel oxide heated to 1450 °C in run 1 results in a thermally stable state. No change appeared in the TG–DTA curves of runs 2 and 3.

Figure 2 shows the results of the stepwise tests on basic nickel carbonate. The ETA peaks corresponding to the decomposition disappear on heating to

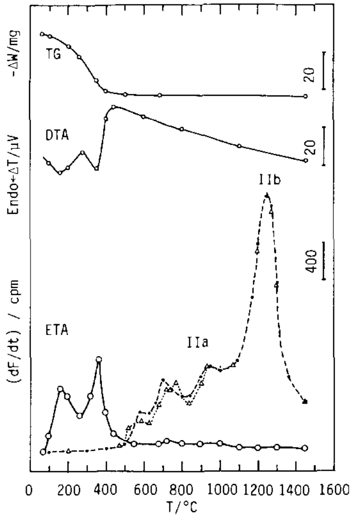

Fig. 1. ETA–TG–DTA curves of basic nickel carbonate: o———o, run 1; ●— — —●, run 2; △- - - - - -△, run 3.

500 °C, and peak IIa (including peak I) is successively shifted to the higher temperature region with heat treatment; finally, the curve leads to peak IIb with a maximum at about 1250 °C with a reduced peak IIa remaining.

Figures 3A and 3B show the ETA curves of two nickel oxides, NiO(C-500) and NiO(C-850), prepared from basic nickel carbonate by calcining for 1 h in air at 500 °C (A) and 850 °C (B). The variation in ETA peak IIa with different heat treatments can be seen, corresponding to the thermal behaviour in Figs. 1 and 2. Peak IIa for all samples finally approaches peak IIb (maximum at 1250 °C) on heating to 1450 °C.

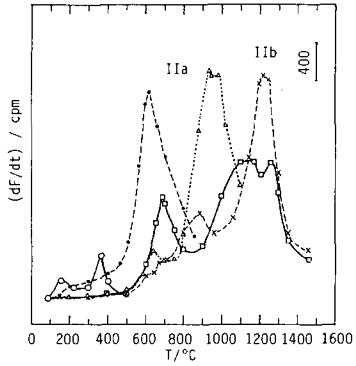

Fig. 2. ETA curves of basic nickel carbonate in stepwise tests. o———o, run 1 (to 500 °C); ●— — —●, run 2 (to 850 °C); △- - - - - -△, run 3 (to 1100 °C); □———□, run 4 (to 1450 °C); × — — — ×, run 5 (to 1450 °C).

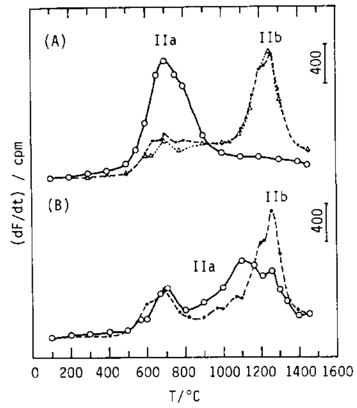

Fig. 3. ETA curves of nickel oxides from basic nickel carbonate: (A) NiO(C-500) and (B) NiO(C-850). ○———○, run 1; ●— — —●, run 2; △- - - - - -△, run 3.

Nickel oxides from hydroxide

Figure 4 shows the ETA–TG–DTA curves of nickel hydroxide in the temperature range 25–1450 ° C, including the decomposition process at temperatures below 500 ° C. In run 1, the TG–DTA curves show the decomposition behaviour, with a good correspondence with the ETA peak below 500 ° C. A pronounced peak IIa appears with a maximum at about 1100 ° C and a small shoulder at about 800 ° C. It is interesting that the thermal behaviour of peak IIa is very different from that in Fig. 1. However, in run 2, for nickel oxide, NiO(H-1450), which was formed in run 1, peak IIb with a maximum at 1250 ° C appears in a similar manner as in Figs. 1–3.

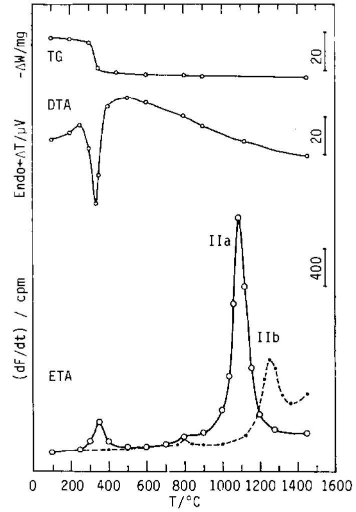

Fig. 4. ETA–TG–DTA curves of nickel hydroxide: ○———○, run 1; ●— — —●, run 2.

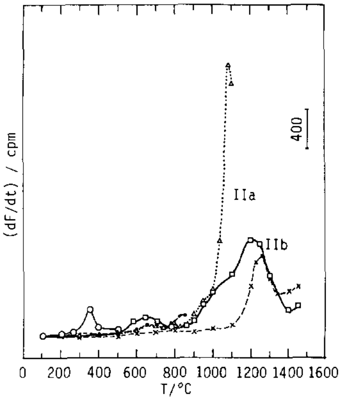

Fig. 5. ETA curves of nickel hydroxide in stepwise tests: ○——○, run 1 (to 500 °C); ●— — —●, run 2 (to 850 °C); △- - - - - -△, run 3 (to 1100 °C); □——□, run 4 (to 1450 °C); × — — — ×, run 5 (to 1450 °C).

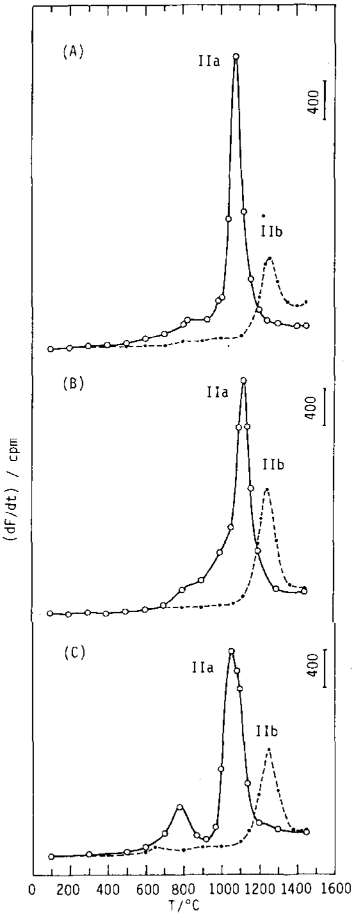

Fig. 6. ETA curves of nickel oxides from nickel hydroxide: (A) NiO(H-500), (B) NiO(H-850) and (C) NiO(H-1100). ○——○, run 1; ●— — —●, run 2.

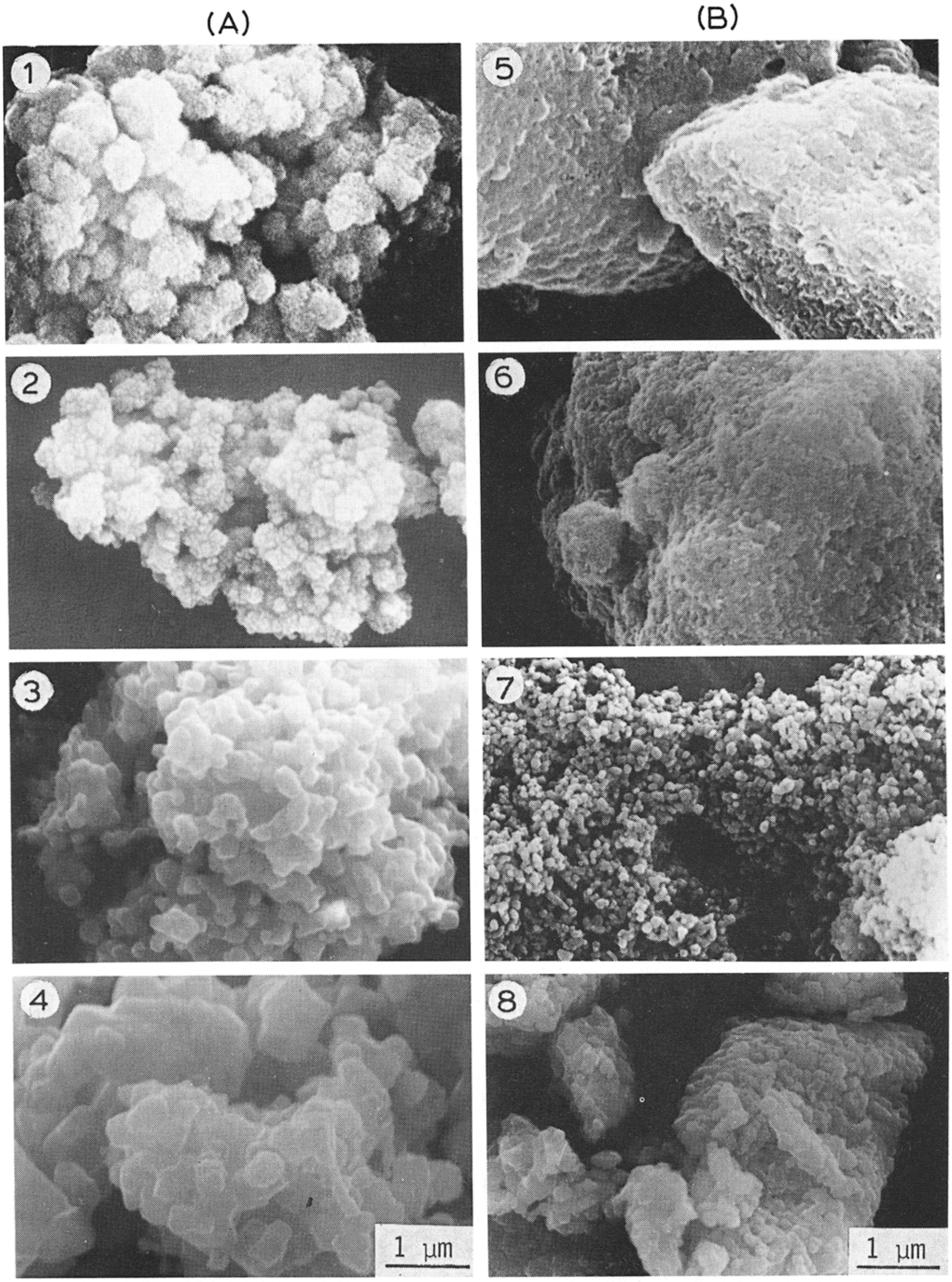

Fig. 7. Scanning electron photomicrographs of nickel oxides in (A) basic nickel carbonate and (B) nickel hydroxide series: (1) basic nickel carbonate, (2) NiO(C-500), (3) NiO(C-850), (4) NiO(C-1100), (5) nickel hydroxide, (6) NiO(H-500), (7) NiO(H-850) and (8) NiO(H-1100). The scale bar applies to all eight photographs.

Figure 5 shows the results of the stepwise tests on nickel hydroxide. In an analogous manner to Fig. 2, the peak corresponding to the decomposition disappears on heating to 500 ° C, peak IIa is successively shifted to the higher temperature region with heat treatments and, finally, the curve leads to peak IIb with a maximum at about 1250 ° C.

Figures 6A–C show the ETA curves for three nickel oxides, NiO(H-500), NiO(H-850) and NiO(H-1100), which were prepared from nickel hydroxide by calcining for 1 h in air at 500 ° C (A), 850 ° C (B) and 1100 ° C (C). In spite of the different heating conditions, the characteristic peaks IIa and IIb largely correspond to those in Figs. 4 and 5. The different thermal behaviour of peak IIa in the nickel oxides of the C and H series is attributable mainly to the different thermal changes of the grain boundaries in two series during the processes directing toward the thermally stable peak IIb.

Figures 7A and 7B show the scanning electron photomicrographs taken at room temperature of the nickel oxides in the C and H series after different heat treatments. The photographs indicate phenomenologically the behaviour of grain growth and the variation in grain boundaries with increasing calcining temperatures. However, it is difficult to characterize the thermal behaviour of the grain boundaries quantitatively from these photographs.

Copper oxides

Copper oxides from carbonate

Figure 8 shows the ETA–TG–DTA curves of basic cupric carbonate in the temperature range 25–800 ° C; the TG curve shows that no decomposition of CuO to Cu_2O occurs. In run 1, the TG–DTA curves show that the decomposition of carbonate to CuO is complete on heating to 500 ° C. In run 2, peak IIa appears, starting at about 450 ° C with a maximum at 600 ° C and a shoulder at 700 ° C. In run 3 (for CuO which was formed in run 2) peak IIa is shifted to the thermally stable peak IIb with a small shoulder at 700 ° C. The curve in run 4 agrees with that in run 3.

Figure 9 shows the ETA–TG–DTA curves of basic cupric carbonate in the temperature range 25–1050 ° C. The TG–DTA curves show that the decomposition of carbonate to CuO is complete on heating to 550 ° C (run 1), and that decomposition of CuO to Cu_2O starts at about 900 ° C (run 2). The ETA peak IIb in run 3 corresponds to that of Cu_2O. The ETA curve in run 4 agrees with that in run 3. The initial appearance of peak IIb for Cu_2O is similar to that of CuO in Fig. 8.

Figure 10 shows the scanning electron photomicrographs taken at room temperature for basic cupric carbonate (A) and copper oxides prepared from basic cupric carbonate with different heat treatments (B). The photographs indicate phenomenologically the behaviour of grain growth and the variation in grain boundaries with increasing calcining temperatures.

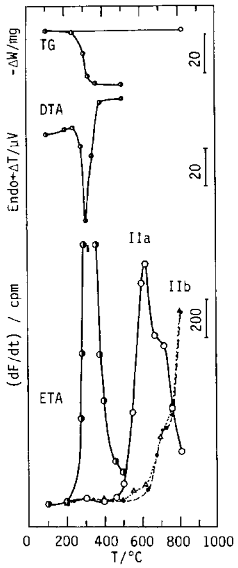

Fig. 8. ETA–TG–DTA curves of basic cupric carbonate in the temperature range 25–800 °C: ◑———◑, run 1 (to 500 °C); ○———○, run 2 (to 800 °C); ●— — —●, run 3 (to 800 °C); △- - - - -△, run 4 (to 800 °C).

Magnesium oxides

Magnesium oxide from carbonate

Figure 11 shows the ETA–TG–DTA curves of basic magnesium carbonate in the temperature range 25–1500 °C, including the decomposition processes

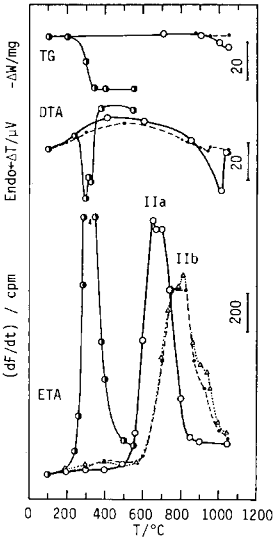

Fig. 9. ETA–TG–DTA curves of basic cupric carbonate in the temperature range 25–1050 °C: ◑———◑, run 1 (to 500 °C); ○———○, run 2 (to 1050 °C); ●— — —●, run 3 (to 1050 °C); △- - - - -△, run 4 (to 1050 °C).

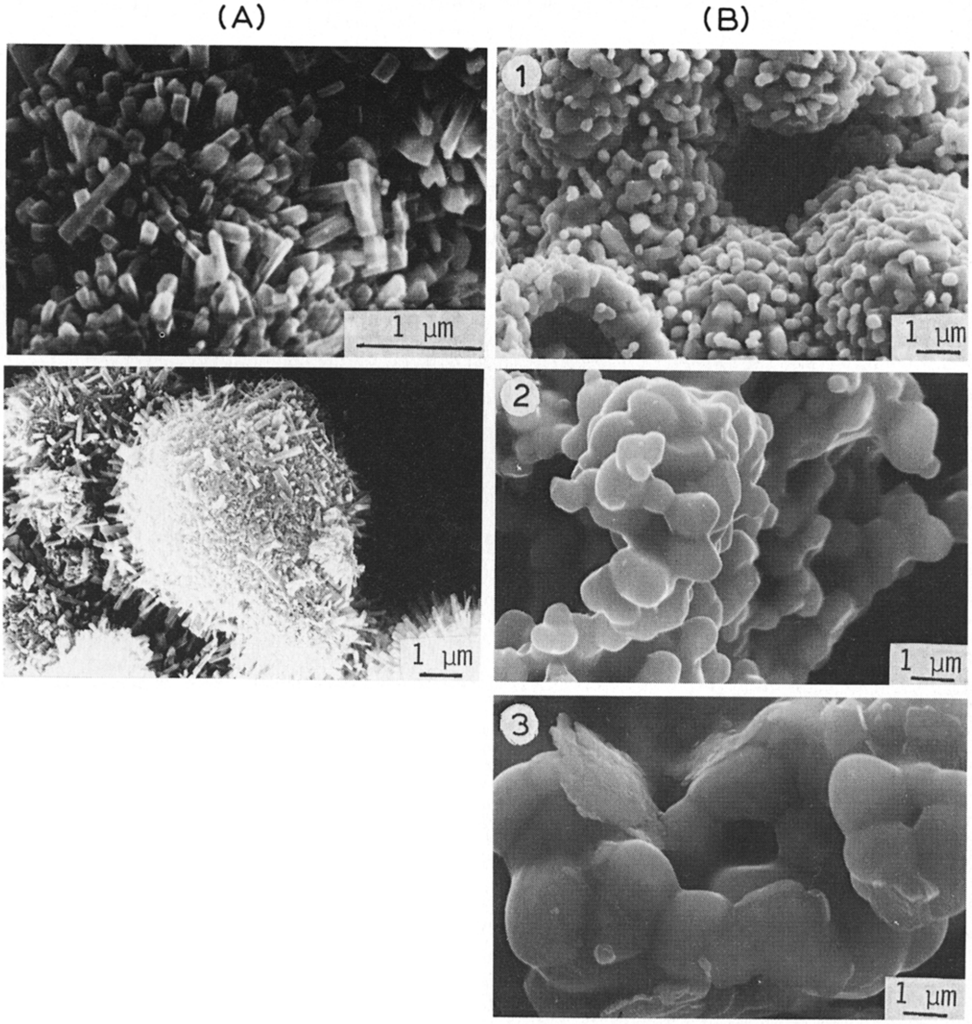

Fig. 10. Scanning electron photomicrographs of (A) basic cupric carbonate and (B) copper oxides prepared from basic cupric carbonate by calcining for 1 h in air at (1) 700 °C, (2) 800 °C and (3) 900 °C.

at temperatures below 600 °C. In run 1, TG–DTA curves show the decomposition behaviour with a good correspondence with the ETA peaks. In ETA run 2 (for magnesium oxide which was formed in run 1) the ETA peaks below 600 °C disappear, and three peaks, I, I′ and II with maxima at about 850, 1150 and 1400 °C, appear. In run 3, the ETA curve agrees with that in run 2. No change appeared in the TG–DTA curves of runs 2 and 3.

Magnesium oxide from hydroxide

Figure 12 shows the ETA–TG–DTA curves of magnesium hydroxide in the temperature range 25–1500 °C, including the decomposition process at temperatures below 600 °C. In run 1, the TG–DTA curves show the

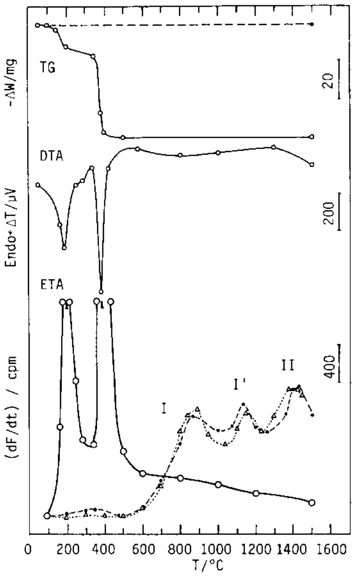

Fig. 11. ETA–TG–DTA curves of basic magnesium carbonate: o———o, run 1; ●— — —●, run 2; △- - - - - -△, run 3.

decomposition behaviour with a good correspondence with the ETA peaks below 600 ° C. Peak I′ is much emphasized compared with that in Fig. 11. It is speculated that this is due to the distinction between the defect structures such as the amorphous product formed during the decomposition processes

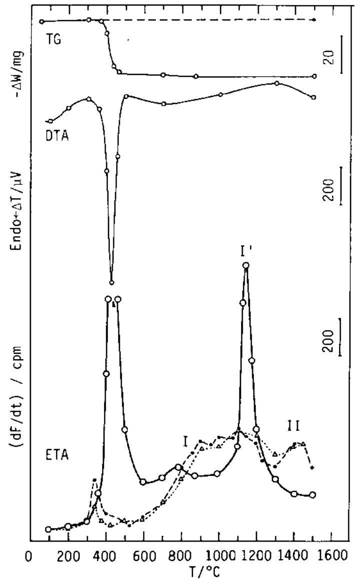

Fig. 12. ETA–TG–DTA curves of magnesium hydroxide: o———o, run 1; ●— — —●, run 2; △- - - - - -△, run 3.

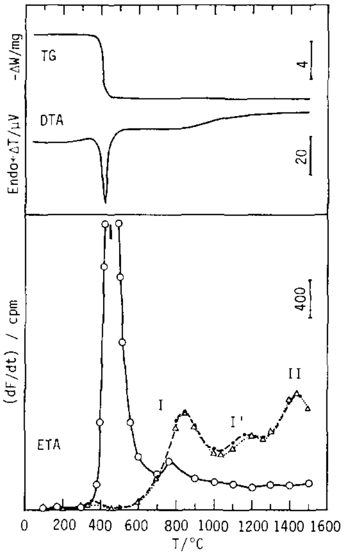

Fig. 13. ETA–TG–DTA curves of commercial magnesium oxide: ○———○, run 1; ●— — —●, run 2; △- - - - -△, run 3.

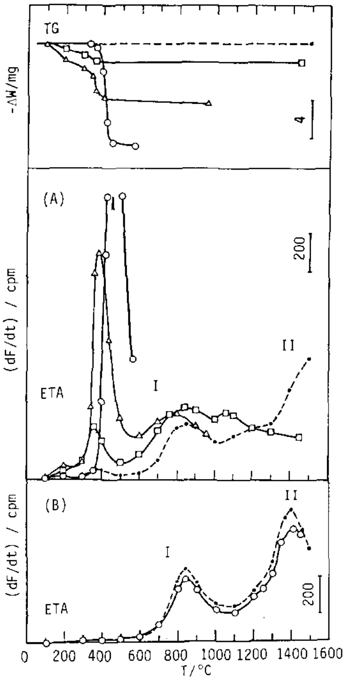

Fig. 14. ETA–TG curves of commercial magnesium oxide in stepwise tests. (A): ○———○, run 1 (to 600 °C); △———△, run 2 (to 950 °C); □———□, run 3 (to 1450 °C); ●— — —●, run 4 (to 1500 °C). (B): ○———○, run 5 (to 1450 °C); ●— — —●, run 6 (to 1500 °C).

of the carbonate and hydroxide. In run 2, the ETA curve becomes similar to that in Fig. 11. In run 3, the ETA curve agrees with that in run 2. No change appeared in the TG–DTA curves of runs 2 and 3.

Commercial magnesium oxide

Figure 13 shows the ETA–TG–DTA curves of commercial magnesium oxide in the temperature range 25–1500 °C. In run 1, the curves below 600 °C show that the sample has been hydrated by the ^{226}Ra aqueous solution in the labelling process. The ETA curves in runs 2 and 3 become similar to those in Figs. 11 and 12.

Figure 14 shows the results of the stepwise tests on magnesium oxide. The TG curves in runs 2 and 3 show that the surface layer of the oxide sample has been acted on by the water vapour and carbon dioxide in the air during the period of storage to achieve radioactive equilibria. No change in the TG curve in run 4 shows that the surface was deactivated when the sample was heated to 1450 °C in run 3. The ETA results show that peak I is gradually shifted to the thermally stable peak II in runs 5 and 6 with heat treatment. However, no pronounced variation appears, compared with the other oxides shown previously. This may be due to the higher melting temperature of magnesium oxide.

CONCLUSIONS

ETA is an interesting technique for studying the thermal characterization of the near-surface of powders at high temperatures, and provides useful information on the thermal behaviour of grain boundaries of polycrystalline metal oxides, which cannot be followed by conventional means such as TG, DTA, XRD, etc.

ACKNOWLEDGEMENTS

The author thanks Mr A. Shimizu for help with ETA studies and Messrs K. Matsui, Y. Tsutsui and T. Sasaki for SEM studies. The ETA studies were carried out at the Central Institute of Isotope Science, Hokkaido University (Sapporo, Japan), and were supported by the Government Science Research fund of the Ministry of Education, Science and Culture of Japan.

REFERENCES

1 T. Ishii, Thermochim. Acta, 88 (1985) 277.
2 T. Ishii, Thermochim. Acta, 93 (1985) 469.

3 T. Ishii, Thermochim. Acta, 109 (1986) 227.
4 T. Ishii, React. Solids, 3 (1987) 85.
5 T. Ishii, React. Solids, 4 (1988) 327.
6 V. Balek, Thermochim. Acta, 22 (1978) 1.
7 T. Hashimoto, Y. Aoyagi, H. Kudo and T. Sotobayashi, J. Radioanal. Nucl. Chem., Articles, 90 (2) (1985) 415.
8 V. Balek, J. Mater. Sci., 17 (1982) 1269.
9 Hj. Matzke, Can. J. Phys., 46 (1968) 621.
10 C. Jech and R. Kelly, Proc. Br. Ceram. Soc., 9 (1967) 259.